

1 **Repurposing tofacitinib as an anti-myeloma therapeutic to reverse growth-promoting**
2 **effects of the bone marrow microenvironment**

3

4 Christine Lam^{1,2}, Megan Murnane^{2,3}, Hui Liu^{1,2}, Geoffrey A. Smith⁴, Sandy Wong^{2,3}, Jack
5 Taunton⁴, Jun O. Liu⁵, Constantine S. Mitsiades⁶, Byron C. Hann², Blake T. Aftab^{2,3}, Arun P.
6 Wiita^{1,2,*}

7

8 ¹Department of Laboratory Medicine, University of California, San Francisco, CA, USA

9 ²Helen Diller Family Comprehensive Cancer Center, University of California, San
10 Francisco, CA, USA

11 ³Department of Medicine, University of California, San Francisco, CA, USA

12 ⁴Department of Cellular and Molecular Pharmacology, University of California, San
13 Francisco, CA, USA

14 ⁵Department of Pharmacology and Molecular Sciences, Johns Hopkins School of
15 Medicine, Baltimore, MD, USA

16 ⁶Department of Medical Oncology, Dana-Farber Cancer Institute, Boston, MA, USA

17

18 **To whom correspondence should be addressed:*

19 Arun P. Wiita, MD, PhD

20 University of California, San Francisco

21 Dept. of Laboratory Medicine

22 185 Berry St, Suite 290

23 San Francisco, CA 94017, USA

24 Tel: 415-514-6238

25 arun.wiita@ucsf.edu

26

27

28 **Abstract**

29 The myeloma bone marrow microenvironment promotes proliferation of malignant plasma cells
30 and resistance to therapy. Interleukin-6 (IL-6) and downstream JAK/STAT signaling are thought
31 to be central components of these microenvironment-induced phenotypes. In a prior drug
32 repurposing screen, we identified tofacitinib, a pan-JAK inhibitor FDA-approved for rheumatoid
33 arthritis, as an agent that may reverse the tumor-stimulating effects of bone marrow
34 mesenchymal stromal cells. Here, we validated both *in vitro*, in stromal-responsive human
35 myeloma cell lines, and *in vivo*, in orthotopic disseminated murine xenograft models of
36 myeloma, that tofacitinib showed both single-agent and combination therapeutic efficacy in
37 myeloma models. Surprisingly, we found that ruxolitinib, an FDA-approved agent targeting
38 JAK1 and JAK2, did not lead to the same anti-myeloma effects. Combination with a novel
39 irreversible JAK3-selective inhibitor also did not enhance ruxolitinib effects. RNA-seq and
40 unbiased phosphoproteomics revealed that marrow stromal cells stimulate a JAK/STAT-
41 mediated proliferative program in myeloma plasma cells, and tofacitinib reversed the large
42 majority of these pro-growth signals. Taken together, our results suggest that tofacitinib
43 specifically reverses the growth-promoting effects of the tumor microenvironment through
44 blocking an IL-6-mediated signaling axis. As tofacitinib is already FDA-approved, these results
45 can be rapidly translated into potential clinical benefits for myeloma patients.

46

47

48 **Introduction**

49 Multiple myeloma (MM) is the second-most common hematologic malignancy in the United
50 States and still has no known cure. A major therapeutic challenge in MM is that patients
51 undergo numerous cycles of response to therapy followed by disease relapse after the
52 development of resistance. Years of research have revealed that a major driver of malignant
53 plasma cell proliferation, as well as therapeutic resistance, is signaling to the tumor cells from
54 the bone marrow microenvironment (reviewed in refs. 1-3). Cell types within the bone marrow
55 that influence myeloma plasma cells include mesenchymal stromal cells, osteoblasts, osteoclasts,
56 and multiple classes of immune cells¹⁻³. Overcoming the growth-promoting phenotype of the
57 bone marrow microenvironment is thought to be a promising therapeutic strategy in MM.

58 One approach to identifying new therapeutic agents for many diseases is drug repurposing.
59 In this context, a large library of drugs, all of which are either FDA-approved or at the minimum
60 shown to be safe in humans, is screened against the biological system of interest^{4,5}. The premise
61 behind these screens is that small molecules initially designed for one indication may actually
62 have beneficial effects across other diseases. In fact the use of thalidomide in multiple myeloma
63 is one of the most impactful examples of successful drug repurposing. If new indications are
64 found for already existing drugs, clinical development times and associated costs can be
65 drastically reduced, accelerating potential benefits to patients^{6,7}.

66 To identify agents which may reverse the tumor-promoting effects of the MM bone marrow
67 microenvironment, we recently reported a repurposing screen of 2,684 compounds, against three
68 MM cell lines, either grown alone (monoculture) or in co-culture with MM patient-derived bone
69 marrow mesenchymal stromal cells⁸. From that screen, we identified tofacitinib citrate, an FDA-
70 approved small molecule for the treatment of rheumatoid arthritis (RA), sold under the trade

71 name Xeljanz, as an agent which may reverse stromal-induced growth proliferation of malignant
72 plasma cells.

73 Tofacitinib citrate is a potent inhibitor of all four members of the Janus kinase (JAK) family,
74 with preferential inhibition of JAK1 and JAK3 over JAK2 and TYK2 in cellular assays⁹. JAK
75 signaling, mediated by the downstream STAT transcription factors, is necessary for lymphocyte
76 stimulation in response to encountered antigens¹⁰. Therefore, JAK inhibition holds promise for
77 the treatment of autoimmune diseases like RA¹¹. In parallel, the JAKs have gained interest as
78 therapeutic targets in MM as they mediate signaling via interleukin-6 (IL-6). IL-6 is secreted by
79 many cell types within the bone marrow microenvironment, as well as by malignant plasma cells
80 themselves, and it is thought that proliferation of malignant plasma cells within the human bone
81 marrow is dependent on this cytokine¹². This dependence on IL-6 was underscored by the recent
82 development of a patient-derived xenograft model of MM, where primary plasma cell growth
83 only occurred in immunocompromised mouse bone marrow after knock-in of human IL-6¹³.

84 Therefore, abrogating IL-6 signaling via JAK inhibition is a promising therapeutic strategy in
85 MM¹⁴. In fact, a number of groups have aimed to target IL-6 stimulation via novel small
86 molecule inhibitors that variously target JAK1/JAK2 (ref. 15,16), JAK2 (ref. 17-19), or all four
87 JAKs (ref. 20), with reported preclinical therapeutic efficacy in MM. However, per the registry
88 at clinicaltrials.gov, none of these experimental JAK inhibitors have ever entered into clinical
89 trials with MM as an indication. Therefore, all of these agents are very far from use in MM
90 patients, if they ever become available at all. Here, we demonstrate that the already FDA-
91 approved agent tofacitinib has robust preclinical activity in MM models. We further use RNA-
92 seq and unbiased mass spectrometry-based phosphoproteomics to delineate pro-proliferative
93 signals from the bone marrow stroma and show that they are largely reversed by tofacitinib

94 treatment. Furthermore, we find that an alternate repurposing candidate, the FDA-approved
95 JAK1/2 inhibitor ruxolitinib, surprisingly does not show the same anti-myeloma properties.
96 Therefore, our results support the rapid repurposing of tofacitinib as an anti-myeloma
97 therapeutic, to reverse the pro-growth effects of the bone marrow microenvironment and
98 potentiate the effects of existing myeloma therapies.

99

100 **Materials and Methods**

101 *Cell culture conditions*

102 HS5 and HS27A stromal cell lines were obtained from American Type Culture Collection
103 (ATCC). MM.1S mC/Luc, stably expressing mCherry and luciferase, were generated from
104 parental MM.1S line obtained from ATCC, as previously described²¹. The RPMI8266 mC/Luc,
105 U266 mC/Luc, and JJN3 mC/Luc lines were generated from parental cell lines obtained from the
106 Deutsche Sammlung von Mikroorganismen und Zellkulturen (DSMZ) repository. These cell lines
107 were stably transduced with a lentiviral expression plasmid constitutively expressing luciferase
108 and mCherry, generated and kindly provided by Dr. Diego Acosta-Alvear at UCSF. L363 cell
109 line was also obtained from DSMZ. AMO-1 cells were kindly provided by Dr. Cristoph Driessen
110 at Kantonsspital St. Gallien, Switzerland. KMS11 cells were obtained from JCRB Cell Bank.
111 INA-6 cells were obtained from Dr. Renate Burger at University Hospital Schleswig-Holstein,
112 Germany. All cells, including patient bone marrow mononuclear cells, were maintained in
113 complete media with RPMI-1640 supplemented with 10% FBS (Gemini), 1% penicillin-
114 streptomycin (UCSF), and 2 mM L-Glutamine (UCSF) with 5% CO₂. INA-6 media was
115 supplemented with 50 ng/mL recombinant human IL-6 (ProSpec).

116

117 *MM and BMSC coculture and viability testing*

118 *Dose response:* Cocultures were seeded into 384 well plates (Corning) with the Multidrop Combi
119 (Thermo Scientific). 800 stromal cells were seeded and incubated overnight. 17 hours later, 700
120 myeloma cells were added on top of stromal cells. On the third day, 24 hours after addition of
121 myeloma cells, cocultures were treated with tofacitinib (LC Laboratories), ruxolitinib (Selleck
122 Chemicals), or JAK3i (ref. 22). For drug combination studies, on the fourth day, melphalan
123 (Sigma Aldrich) or carfilzomib (Selleck Chemicals) were additionally added to cocultures. On
124 the fifth day, myeloma cell viability was detected with addition of luciferin (Gold
125 Biotechnology) and read for luminescence on Glomax Explorer plate reader (Promega) as
126 previously described²¹. For monoculture studies cell viability was measured using Cell-Titer Glo
127 reagent (Promega). All measurements were performed in quadruplicate. All viability data are
128 reported as normalized to DMSO-treated cell line in monoculture.

129

130 *RNA-seq*

131 For co-culture RNA-seq, 5×10^6 MM.1S cells were grown in co-culture with 3×10^6 HS5 cells for
132 24 hr. All cells were harvested by Accutase incubation for 10 min at 37 C to separate MM.1S
133 from HS5 into a single-cell suspension. Cells were then separated using CD138+ MicroBeads
134 (Miltenyi) on a Miltenyi MidiMACS system. CD138+ enrichment to >95% was verified by flow
135 cytometry for mCherry expression (Supplementary Fig. 1). MM.1S harvested from co-culture,
136 as well as MM.1S and HS5 grown in monoculture, were then processed for mRNA-seq as
137 previously described²³. RNA-seq performed on HS5 stromal cells alone further allowed for
138 filtering of highly expressed stromal cell genes that could interfere with analysis of MM.1S cells
139 in co-culture even at <5% contamination. Significantly upregulated transcripts were identified

140 by DESeq²⁴ and bioinformatic analysis was performed using Enrichr²⁵. Raw sequencing data are
141 available at the GEO repository (Accession number GSE99293).

142

143 *Western Blot Analysis*

144 For co-culture studies, 3×10^5 HS5 were seeded into 6 well plate. 17 hours later, 5×10^6 MM.1S
145 mC/Luc cells were added on top of stromal cell layer. For monoculture studies 5×10^6 MM1.S
146 cells alone were used. Cells were treated with tofacitinib or ruxolitinib from 0-24 hours and the
147 supernatant, containing all MM1.S cells in suspension, harvested for processing by
148 centrifugation. All Western blots were performed at in biological duplicate with representative
149 blots displayed. pSTAT3 (Tyr705), STAT3, pSTAT1 (Tyr701)(58D6), STAT1,
150 pJAK1(Tyr1022/1023), JAK1, pJAK2 (Tyr1008), JAK2, pJAK3 (Tyr980/981), JAK3, pTYK2
151 (Tyr1054/1055), pSTAT5 (Tyr694), and STAT5 antibodies were purchased from Cell Signaling
152 Technology. Tyk2 antibody was purchased from Santa Cruz Biotechnology. Western blot was
153 carried out as previously described²³.

154

155 *Liquid chromatography–tandem mass spectrometry phosphoproteomics*

156 For co-culture experiments, 5×10^6 HS5 were seeded into a T75 flask. 17 hours later, cultures
157 were washed with PBS, before addition of 10^7 MM.1S mC/Luc cells. 24 hours later, cocultures
158 were treated with 1 μ M tofacitinib for 1.5 hours and 24 hours. On the third day, MM1.S cells in
159 suspension were harvested by aspiration, centrifuged, washed with PBS, and flash-frozen prior to
160 analysis. For untreated MM1.S monoculture experiments 10^7 cells were used. For sample
161 preparation frozen cell pellets were lysed in 8M urea. 1 mg of total protein was then reduced in
162 TCEP and free cysteines alkylated with iodoacetamide. Proteins were then digested at room
163 temperature for 18 hours with trypsin. Peptides were desalted, lyophilized, and enriched for

164 phosphopeptides using immobilized-metal affinity column (IMAC) with Fe-NTA loaded beads²⁶.
165 Phosphopeptides were analyzed on a Thermo Q-Exactive Plus mass spectrometer coupled to a
166 Dionex Ultimate 3000 NanoRSLC liquid chromatography instrument with 3.5 hr linear gradient.
167 Spectra were acquired in data-dependent acquisition mode at 70,000 resolution. Raw mass
168 spectrometry data for two biological replicates were processed using Maxquant v1.5 (ref. 27)
169 versus the Uniprot human proteome (downloaded Feb. 20, 2017; 157,537 entries), with phospho
170 (STY) selected as a fixed modification and match between runs enabled. Only phosphopeptides
171 with measured MaxQuant MS1 intensity in all samples were used for analysis. Median intensity
172 normalization of all phosphopeptides in the sample was performed prior to analysis. Raw
173 proteomic data files are available at the ProteomXchange PRIDE repository (Accession number
174 PXD006581).

175

176 *Xenograft mouse model*

177 NOD.*Cg-Prkdc^{scid} Il2rg^{tm1Wjl}/SzJ* (NSG) mice were obtained from Jackson laboratory. 10⁶
178 MM.1S mC/Luc or U266 mC/Luc, stably expressing luciferase, were transplanted via tail vein
179 injection into each mouse. Tumor burden was assessed through weekly bioluminescent imaging,
180 beginning 13 days after implantation and same day as treatment initiation. Mice were treated for
181 4 weeks with vehicle, tofacitinib, carfilzomib, and combination of tofacitinib and carfilzomib as
182 indicated (5 mice/arm.) Tofacitinib was formulated in 50% DMSO, 10% PEG 400, and 40%
183 water and administered at 21.5 mg/kg daily by continuous subcutaneous infusion. Carfilzomib
184 was formulated in 10% cyclodextrin (Captisol) and 10 mM sodium citrate, pH 3.5, administered
185 at 2 mg/kg 2x/week IV. Vehicle was carfilzomib formulation administered 2x/week IV. All

186 mouse studies were performed according to UCSF Institutional Animal Care and Use
187 Committee-approved protocols.

188

189 *Patient samples*

190 De-identified primary MM bone marrow samples were obtained from the UCSF Hematologic
191 Malignancy Tissue Bank in accordance with UCSF Committee on Human Research-approved
192 protocols. Bone marrow mononuclear cells were isolated by density gradient centrifugation
193 Histopaque-1077 (Sigma Aldrich), then adjusted to 2×10^5 /well in a 96 well plate. Primary cells
194 were stimulated with 50 ng/ml recombinant human IL-6 (ProsPec) for 17 hours before treatment
195 with tofacitinib for 24 hours. Cells were then stained with Alexa-Fluor 647 mouse anti-human
196 CD138 antibody (BD Pharmingen), Alexa-Fluor 647 mouse IgG1, κ isotype control (BD
197 Pharmingen), and Hoechst 33258 (Thermo Fisher Scientific) and analyzed on a FACS Aria
198 instrument (BD).

199

200 **Results**

201 **Tofacitinib targets the BM microenvironment and reverses bone marrow stromal cell-** 202 **mediated growth promotion**

203 To initially validate findings from our drug repurposing screen, we co-cultured the human MM
204 cell line MM.1S, which was included in the screen⁸, with the immortalized bone marrow stromal
205 cell lines HS5 and HS27A. We found that after 24h of co-culture, MM.1S cell numbers
206 approximately doubled compared to monoculture growth after 24h, confirming stromal-induced
207 proliferative signaling in this cell line, as seen in the screen. Tofacitinib treatment for 24 hr
208 reduced MM.1S cell numbers in a dose-dependent manner, such that at $>1 \mu\text{M}$ tofacitinib,

209 MM.1S cell numbers in coculture return to approximately monoculture levels (Fig. 1A).
210 Tofacitinib has no effect on MM.1S cell viability alone nor on HS5 or HS27A alone (Fig. 1B).
211 We further studied the effect of tofacitinib on several other immortalized MM cell lines. In
212 monoculture we found that tofacitinib only demonstrates anti-MM activity in the IL-6 secreting
213 line U266 and in the IL-6 dependent cell line INA-6, with minimal to no effect on the other MM
214 cell lines (Fig. 1C). We further evaluated four myeloma cell lines (U266, MM.1S, RPMI-8226,
215 JLN-3) in which luciferase was stably expressed, allowing for distinction of MM cell viability
216 versus stromal cell viability in co-culture, in the compartment-specific bioluminescence assay²¹.
217 After 24 hr of growth followed by 24 hr of drug exposure, only the stromal-responsive cell lines
218 MM.1S and U266 exhibit any sensitivity to tofacitinib treatment (Fig. 1D). Taken together,
219 these results suggest that tofacitinib selectively targets the growth-promoting interaction between
220 MM cells and the stromal microenvironment. These results further suggest that MM.1S is an
221 appropriate cell line candidate for further study, as it recapitulates the growth-promoting effects
222 of the bone marrow microenvironment known to occur in patients.

223

224 **Tofacitinib inhibits IL-6 driven growth promotion in coculture with bone marrow stromal** 225 **cells**

226 To further characterize the nature of pro-growth signaling between the stromal cell
227 microenvironment and MM plasma cells, we performed RNA-seq on MM.1S cells grown alone
228 or grown in co-culture with HS5 stromal cells. We first noticed that the most significantly
229 upregulated transcript in MM.1S in the co-culture setting was SOCS3, part of a well-
230 characterized negative feedback mechanism strongly induced by JAK-STAT activation¹⁰ (Fig.
231 2A). We further examined all 67 transcripts significantly upregulated in MM.1S in the co-

232 culture vs. monoculture setting ($p < 0.005$ per DESeq tool²⁴; listed in Supplementary Dataset 1).
233 Using the Enrichr tool²⁵, ChEA analysis of ChIP-seq datasets²⁸ found the most significant
234 enrichment of STAT3-binding sites at the promoter of these upregulated transcripts, among all
235 transcription factors (Fig. 2B). Furthermore, Panther²⁹ pathway analysis found the only two
236 significantly enriched pathways to be related to JAK/STAT signaling and interleukin signaling
237 (Fig. 2C). Taken together, these RNA-seq findings are most consistent with a mechanism where
238 IL-6 secreted from stromal cells mediates proliferation by activating JAK/STAT signaling, with
239 STAT3 playing a central role³⁰.

240 We further investigated this mechanism by confirming that MM.1S cells stimulated with
241 50 ng/mL recombinant human IL-6 exhibited growth promotion similar to that induced by
242 coculture with stromal cells, suggesting that IL-6 is the primary cytokine mediating stromal-cell
243 induced proliferation (Fig. 2D). Tofacitinib was capable of partially reversing this IL-6 induced
244 growth promotion in MM.1S at drug concentrations similar to those found for phenotypic effects
245 for stromal cell co-culture. We note that we did not find complete reversal of the growth
246 promotion, however, perhaps indicating that the high doses of recombinant IL-6 used here may
247 lead to residual proliferative signaling not fully blocked by tofacitinib.

248 We further took advantage of publicly available RNA-seq data across a large panel of
249 MM cell lines (<http://www.keatslab.org/data-repository>) to look for relationships between IL-6
250 and IL-6R expression and sensitivity to tofacitinib (Fig. 3E-F). Consistent with prior studies³¹,
251 only U266 expresses detectable levels of IL-6, whereas both U266 and MM.1S express relatively
252 high levels of IL-6R compared to other cell lines examined in Fig. 1, suggesting a relationship
253 between IL-6, IL-6R, and sensitivity to tofacitinib.

254

255 **Tofacitinib inhibits JAK/STAT signaling**

256 Given the proposed mechanism above, we chose to further evaluate downstream effects of IL-6-
257 mediated stimulation and subsequent tofacitinib inhibition of the JAK/STAT pathway. Two of
258 the primary downstream mediators of IL-6R and JAK activation are thought to be pro-
259 proliferation signaling by STAT3 and inhibitory signaling by STAT1³⁰. As expected, we found
260 that STAT3 and STAT1 phosphorylation in MM.1S dramatically increases when in coculture
261 with HS5 (Fig. 3A and 3B). 1 μ M tofacitinib inhibits STAT3 phosphorylation in MM.1S cells in
262 coculture almost to monoculture level by 2 hrs of treatment, suggestive of on-target effects.
263 Phosphorylation of JAK1, JAK2, and TYK2, which can also activate STAT3, were also studied.
264 We found evidence of a “rebound” effect by 24h of treatment, mediated by well-characterized
265 feedback mechanisms¹⁰, serving to phosphorylate the JAKs and subsequently re-activate STAT3.
266 Despite this rebound of STAT3 activation, however, MM growth continues to be inhibited based
267 on dose-response results of tofacitinib treatment at 24 hours.

268 As tofacitinib is known to potently inhibit JAK3, also of interest was an increase in JAK3
269 expression in MM.1S in coculture versus monoculture, found both by RNA-seq (Fig. 2A) and
270 Western blot (Fig. 3C). However, tofacitinib did not lead to any significant decrease in JAK3
271 phosphorylation (Fig. 3C). We also evaluated signaling through JAK3’s primary pro-
272 proliferative downstream mediator STAT5 (ref. 32). We found no evidence of STAT5
273 phosphorylation in either monoculture or co-culture (Supplementary Fig. 2A). These results
274 suggest that JAK3/STAT5 signaling is less central to stroma-supported MM growth. We further
275 confirmed this result using JAK3i, a newly-described, highly-specific, irreversible JAK3
276 inhibitor³². JAK3i had no effect on MM.1S in mono- or coculture (Fig. 4A), nor did it show any
277 synergy with carfilzomib treatment (Supplementary Figure 2B-C).

278 Taken together, these results suggest a mechanism whereby stromal cell-induced MM
279 proliferation is mediated through STAT3 transcriptional effects. These signaling pathways are
280 inhibited in an on-target fashion by tofacitinib, ultimately leading to reversal of the proliferation
281 phenotype.

282

283 **Ruxolinitib has less anti-MM activity than tofacitinib**

284 Given that our results above suggest a more important role for JAK1 and/or JAK2 in stromal-
285 induced MM proliferation than JAK3, we turned to an alternate candidate for drug repurposing,
286 ruxolinitib. This agent, sold under the trade name Jakofi, is FDA-approved for use in
287 myeloproliferative neoplasms and has much higher affinity for JAK1 and JAK2 over JAK3 or
288 TYK2 (ref. 33). Treatment of U266 cells showed some anti-myeloma effect (Fig. 4B-C) but this
289 was significantly reduced compared to tofacitinib (Fig. 1). Surprisingly, treatment of MM.1S
290 actually showed a promotion of growth at higher concentrations, both in the monoculture and co-
291 culture settings (Fig. 4B-C). Western blotting demonstrated that 1 μ M ruxolinitib was unable to
292 inhibit STAT3 activation in MM.1S in co-culture (Fig. 4D). In fact, STAT3 phosphorylation
293 increased after 2 hr of treatment, consistent with the pro-proliferative effect seen in Fig. 4B-C.
294 To confirm that these effects could not be rescued with simultaneous inhibition of JAK1/2/3, as
295 accomplished by tofacitinib, we combined ruxolinitib with JAK3i. We found this combination
296 was also insufficient to recapitulate tofacitinib's effects in mono- or co-culture (Fig. 4E-F).
297 Taken together, these findings suggest that ruxolinitib is unable to inhibit pro-proliferative
298 STAT3 signaling in an in MM.1S cells, thereby supporting tofacitinib as having greater potential
299 as a repurposed anti-myeloma therapy.

300

301 **Unbiased phosphoproteomics demonstrates that tofacitinib broadly reverses pro-growth**
302 **signaling induced by bone marrow stroma**

303 Our targeted investigations above specifically focused on the JAK/STAT pathway. To further
304 elucidate the mechanism of tofacitinib in this system, as well as gain a broader view of stromal-
305 induced proliferation and signaling in MM cells, we pursued unbiased mass spectrometry (MS)-
306 based phosphoproteomics. We studied four samples, performed in biological replicate: 1)
307 MM.1S cells in monoculture; MM.1S cells in co-culture, either 2) untreated (DMSO control); 3)
308 treated with 1 μ M tofacitinib for 1.5 hr; or 4) treated with 1 μ M tofacitinib for 24 hr. We
309 harvested MM.1S cells in suspension, enriched for phosphorylated peptides using immobilized
310 metal chromatography, and analyzed by LC/MS-MS with peptide quantification performed using
311 MaxQuant²⁷.

312 In total 4862 phosphopeptides had intensity data in all four samples and were used for
313 further analysis (listed in Supplementary Dataset 2). >99% of these sites are serine and threonine
314 phosphorylation events, consistent with other phosphoproteomic studies using this enrichment
315 method³⁴. We first evaluated for phosphosites with >4-fold intensity increases in untreated co-
316 culture vs. monoculture. Using our RNA-seq data as a proxy for protein-level changes, we
317 verified these phospho-site changes were largely driven by changes in signaling and not protein
318 abundance (Supplementary Fig. 3). Panther pathway analysis revealed the only significantly
319 enriched pathway among the 544 upregulated phosphosites to be JAK/STAT signaling (Fig. 5A).
320 However, based on Kinase Enrichment Analysis³⁵, we found enriched signatures not only of
321 JAK1 substrates, but also other kinases driving proliferation and the cell cycle such as mTOR,
322 CDK1, and CDK2 (Fig. 5B). These findings demonstrate that unbiased phosphoproteomics can

323 uncover broad signaling effects of the bone marrow microenvironment even downstream of
324 JAK/STAT.

325 Next, for validation of effects of tofacitinib treatment, we first examined Ser727 on
326 STAT3 (Fig. 5C), a known JAK-responsive phosphosite³⁰. Our quantitative MS results were
327 remarkably in line with Western blotting for another JAK-responsive phosphosite on STAT3,
328 Tyr707 (Fig. 3A), with a very large increase in both phosphosites in untreated co-culture
329 compared to baseline, a >2-fold decrease in phosphorylation after short-term tofacitinib
330 treatment, and a rebound in phosphorylation at 24 hr.

331 This finding both serves to validate our phosphoproteomic data as well as help us define
332 a signature of tofacitinib-responsive phosphosites. Remarkably, 336 of the 544 up-regulated
333 phosphosites in untreated co-culture vs. monoculture (62%) met the same criteria of being
334 tofacitinib-responsive (Fig. 5D-E). Furthermore, examination across all measured phosphosites
335 demonstrates that while phosphorylation is broadly increased in the co-culture setting, noted as a
336 general shift toward positive phosphosite intensities in the untreated sample, treatment with
337 tofacitinib largely reverses this finding, re-creating a normal distribution around the intensity
338 values found in monoculture (Fig. 5F). Taken together, these findings demonstrate that
339 tofacitinib broadly reverses the signaling pathways driving stromal-included proliferation in MM
340 cells, both at the level of direct JAK targets as well downstream proliferative signals, informing
341 our mechanistic understanding of this treatment beyond targeted Western blots alone.

342

343 **Tofacitinib does not appear to have significant off-target activity**

344 Another advantage of unbiased phosphoproteomics is potentially detecting additional off-
345 target effects mediating tofacitinib response. We filtered for peptides that appeared unaffected

346 by stromal-induced signaling (less than +/- 50% intensity change in untreated co-culture vs.
347 monoculture) that decreased in intensity >4-fold after 1.5 hr tofacitinib treatment (Fig. 6A). We
348 identified only 54 peptides that fit this filter, and neither Panther nor Kinase Enrichment
349 Analysis identified any enriched signatures (not shown). Given the small number of peptides
350 and lack of any biological signatures, it appears most likely these 54 peptides are background
351 noise in the data and do not suggest any significant off-target effects of tofacitinib.

352 However, to further investigate the possibility of any off-target effects of tofacitinib, we
353 downloaded available data from the LINCS KINOMEscan database
354 (<http://lincs.hms.harvard.edu/kinomescan/>) and plotted versus the human kinase phylogenetic
355 tree (Fig. 6B). These results demonstrate that, at least in cell-free assays, tofacitinib shows much
356 greater specificity for JAK-family kinases compared to ruxolitinib, which has numerous off-
357 target activities. These findings underscore that tofacitinib's effects in this co-culture model
358 appear to be due to on-target activity. Furthermore, we speculate that through an as-yet-
359 undefined mechanism, off-target effects of ruxolitinib may antagonize on-target JAK/STAT
360 inhibition in these MM models, leading to decreased efficacy of ruxolitinib compared to
361 tofacitinib.

362

363 **Tofacitinib has anti-MM activity in the bone marrow microenvironment *in vivo***

364 Toward the goal of repurposing tofacitinib as an anti-MM therapy in patients, we next examined
365 the efficacy of tofacitinib *in vivo*. For this orthotopic disseminated xenograft model we used
366 luciferase-labeled MM.1S and U266 cell lines, which specifically home to the murine bone
367 marrow after intravenous implantation in NOD *scid* gamma (NSG) mice. Treatment was
368 initiated after two weeks of tumor growth and continued for four weeks at ~2/3 of the maximal

369 tolerated dose of tofacitinib (21.5 mg/kg/day by subcutaneous infusion)³⁶. Encouragingly, we
370 found significantly increased murine survival in both of these cell line models (Fig. 7A-B) as
371 well as decreased tumor burden based on bioluminescent imaging quantification (Fig. 7C-D).
372 These findings indicate that despite the *in vitro* rebound we observed in STAT3 activation (Fig.
373 3A), continuous treatment with tofacitinib still leads to anti-myeloma effects *in vivo*.

374 We also performed *in vitro* studies of tofacitinib in combination with first-line myeloma
375 therapies carfilzomib and melphalan (Supplementary Fig. 4). We found combination effects
376 with both of these agents in the co-culture model. Based on these results, in our U266 murine
377 study we also included study arms with carfilzomib alone at 2/3 of the maximal tolerated dose (2
378 mg/kg IV, 2x/week) and a combination of carfilzomib and tofacitinib at the above doses. We
379 found that tofacitinib led to similar lifespan extension as carfilzomib monotherapy, and also
380 found evidence of additive effects of the two agents, though the difference between the
381 combination and either monotherapy was not statistically significant.

382 We also tested tofacitinib versus two primary MM bone marrow samples treated *ex vivo*.
383 We did not see any significant viability effects of tofacitinib in either of these samples, against
384 either malignant plasma cells or other normal bone marrow mononuclear cells (Supplementary
385 Fig. 5). However, this result appears consistent with our *in vitro* and phosphoproteomic results,
386 which suggest that IL-6 dependent plasma cell proliferation is necessary for tofacitinib to have
387 any effect. Primary MM plasma cells isolated *ex vivo* in 2D culture are known to have minimal
388 ability to actively proliferate even in the presence of cytokines or stromal stimulation³⁷.
389 Therefore, these results may more reveal the limitations of *ex vivo* patient assays in MM rather
390 than preclude the therapeutic efficacy of tofacitinib in MM patients, where plasma cells are
391 constantly proliferating in an IL-6-dependent manner within the bone marrow.

392

393 **Discussion**

394 Given the importance of the bone marrow microenvironment for MM pathogenesis, the
395 IL-6/JAK/STAT signaling axis has generated significant interest as a therapeutic target in MM.
396 JAK inhibition has already been validated in a number of preclinical studies as a way to target
397 this pathway¹⁵⁻²⁰. However, the studied compounds are not yet available clinically and may
398 never be. Here, following the results of a large scale repurposing screen, we validated tofacitinib
399 as a potential therapy that can be rapidly translated into MM patients.

400 Using a combination of mechanistic pharmacology and unbiased mass spectrometry-
401 based phosphoproteomics, we found that tofacitinib appears to inhibit stromal-induced
402 proliferation of MM plasma cells by inhibiting the IL-6/JAK/STAT signaling axis. Our results
403 support the use of unbiased phosphoproteomics both in kinase inhibitor evaluation and more
404 broadly in MM biology, where this method has been only applied in a very limited fashion.

405 Surprisingly, in our studies we found that the FDA-approved JAK1/2 inhibitor ruxolitinib
406 did not lead to the same anti-myeloma effects as tofacitinib, and in fact may paradoxically
407 promote plasma cell proliferation at high concentrations. We do note that ruxolitinib was
408 previously evaluated in a small trial of 13 MM patients in combination with dexamethasone
409 (NCT00639002) and no significant anti-MM effects were noted in this small study. Our *in vitro*
410 results here may provide a partial explanation for the lack of ruxolitinib activity in that trial.

411 We note that these studies are of course limited in that they are performed in MM cell
412 lines. While we primarily focused our analysis on the stromal-responsive cell lines MM.1S and
413 U266, which appear to better mimic the malignant plasma cell phenotype found in MM patients,

414 at this point focused clinical trials in MM will be necessary to truly evaluate whether tofacitinib
415 has anti-MM effects.

416 Toward this goal, the value of drug repurposing becomes readily apparent. Tofacitinib
417 can be quickly moved into Phase I/II studies in MM as the tolerated doses and adverse event
418 profiles of this drug are well-characterized in humans¹¹. Tofacitinib is generally well-tolerated at
419 therapeutic doses in RA¹¹ and, despite early concerns, post-market surveillance studies have not
420 revealed any increased risk of malignancies compared to other RA therapies³⁸. Intriguingly, a
421 patient population with both MM and RA could readily serve as the basis of a multi-center trial
422 in combination with standard of care MM therapies. Alternatively, a patient population with
423 early-stage disease, perhaps smoldering myeloma, may be the optimal setting for clinical use,
424 when plasma cells may be most dependent on IL-6 and other microenvironment cues. In
425 conclusion, tofacitinib is a promising agent to reverse the tumor-proliferative effects of the bone
426 marrow microenvironment that can be rapidly repurposed to benefit MM patients.

427

428 **Acknowledgements**

429 This work was supported by the UCSF Stephen and Nancy Grand Multiple Myeloma
430 Translational Initiative and The Myeloma Research Fund of the Silicon Valley Community
431 Foundation (to B.T.A. and A.P.W.), and an NCI Clinical Scientist Development Award (K08
432 CA184116), a Dale F. Frey Breakthrough Award from the Damon Runyon Cancer Research
433 Foundation (DFS 14-15), and an American Cancer Society Individual Research Award (IRG-97-
434 150-13) (to A.P.W.). We thank Drs. Jeffrey Wolf, Tom Martin, Nina Shah, and Cammie
435 Edwards for discussions, advice, and insight. We thank the staff of the UCSF Helen Diller
436 Family Cancer Center Preclinical Therapeutic Core facility, supported by NCI Cancer Center

437 Support Grant P30 CA082103, for completion of murine studies. We thank Dr. Diego Acosta-

438 Alvear for providing luciferase-labeled MM cell lines.

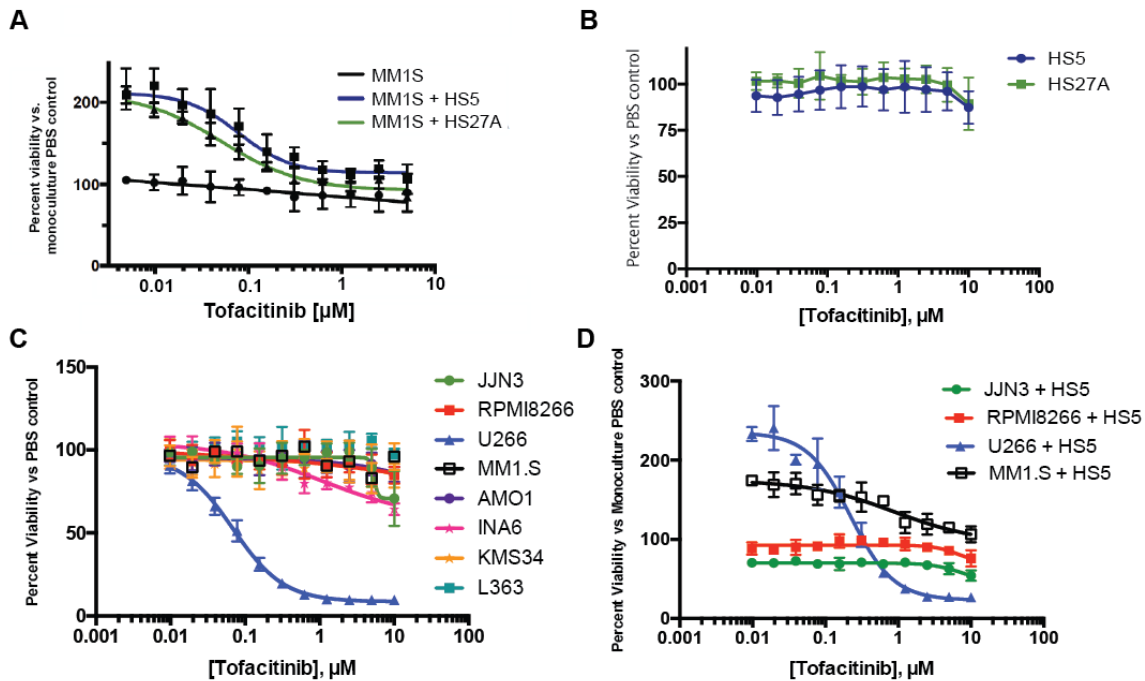
439

440

441

442 **FIGURES**

443



444

445 **Figure 1. Tofacitinib inhibits stromal-cell proliferation in MM cells mediated by IL-6. A.**

446 Tofacitinib has no effect vs. MM1S MM cells in monoculture but instead reverses proliferation

447 induced by bone marrow stromal cell lines HS5 and HS27A. **B.** Tofacitinib has no viability

448 effect vs. bone marrow stromal cells. **C.** Tofacitinib has minimal effects vs. most MM cell lines

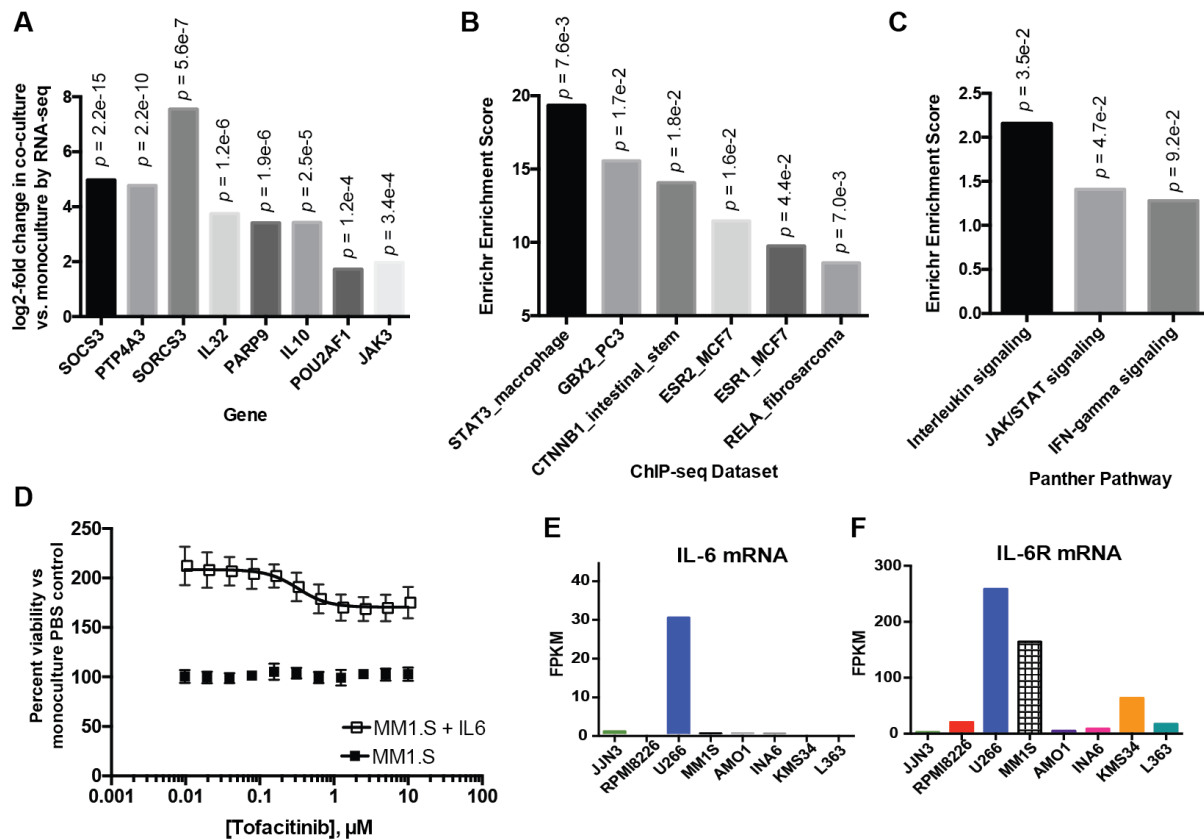
449 in mono-culture, except the IL-6 secreting line U266 and IL-6 dependent line INA-6. **D.** In

450 stromal cell co-culture, tofacitinib does not have anti-MM effects vs. JYN-3 and RPMI-8226 cell

451 lines, which do not proliferate in response to stroma. All error bars represent +/- S.D. from assay

452 performed in quadruplicate in 384-well plates.

453



454

455 **Figure 2. Stromal-induced signatures in MM.1S identified by transcriptome analysis. A.**

456 Examples of significantly upregulated genes in MM.1S cells co-cultured with HS5 stromal

457 cells in comparison to MM.1S grown in monoculture. **B.** ChEA analysis of 72 significantly

458 upregulated transcripts from untreated MM.1S in HS5 co-culture vs. monoculture ($p < 0.05$

459 based on DESeq analysis) demonstrates a significant enrichment of STAT3 transcription-factor

460 binding sites based on ChIP-seq data. **C.** Panther pathway analysis of this gene list

461 demonstrates significant upregulation of interleukin signaling and JAK-STAT signaling among.

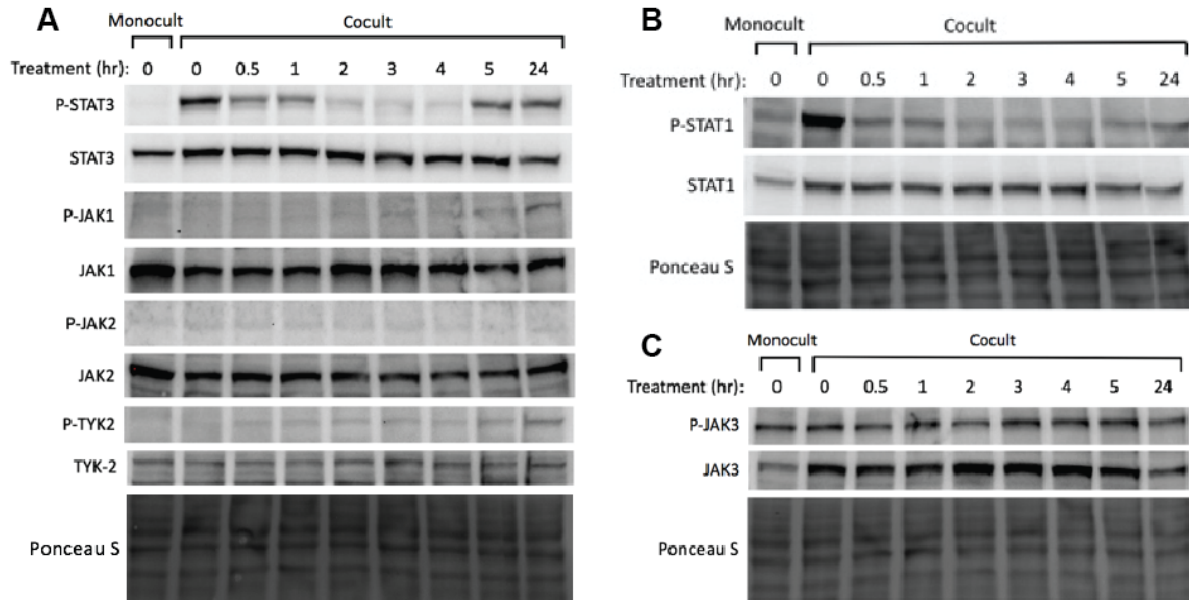
462 **D.** Tofacitinib reverses proliferation induced by recombinant IL-6 in MM.1S (50 ng/mL). Error

463 bars represent +/- S.D. from assay performed in quadruplicate in 384-well plates. **E.-F.**

464 Analysis of cross-cell-line RNA-seq data at <http://www.keatslab.org/data-repository>

465 demonstrates a potential relationship between IL-6 and/or IL-6R gene expression and sensitivity

466 to tofacitinib.



467

468 **Figure 3. Tofacitinib inhibits JAK/STAT signaling in MM cells in a time-dependent**

469 **manner. A.** Western blotting demonstrates a marked increase in STAT3 phosphorylation in

470 untreated co-culture vs. monoculture in MM.1S cells. After treatment with 1 μ M tofacitinib

471 there is a rapid decrease in STAT3 phosphorylation with rebound by 24 hr. **B.** STAT1

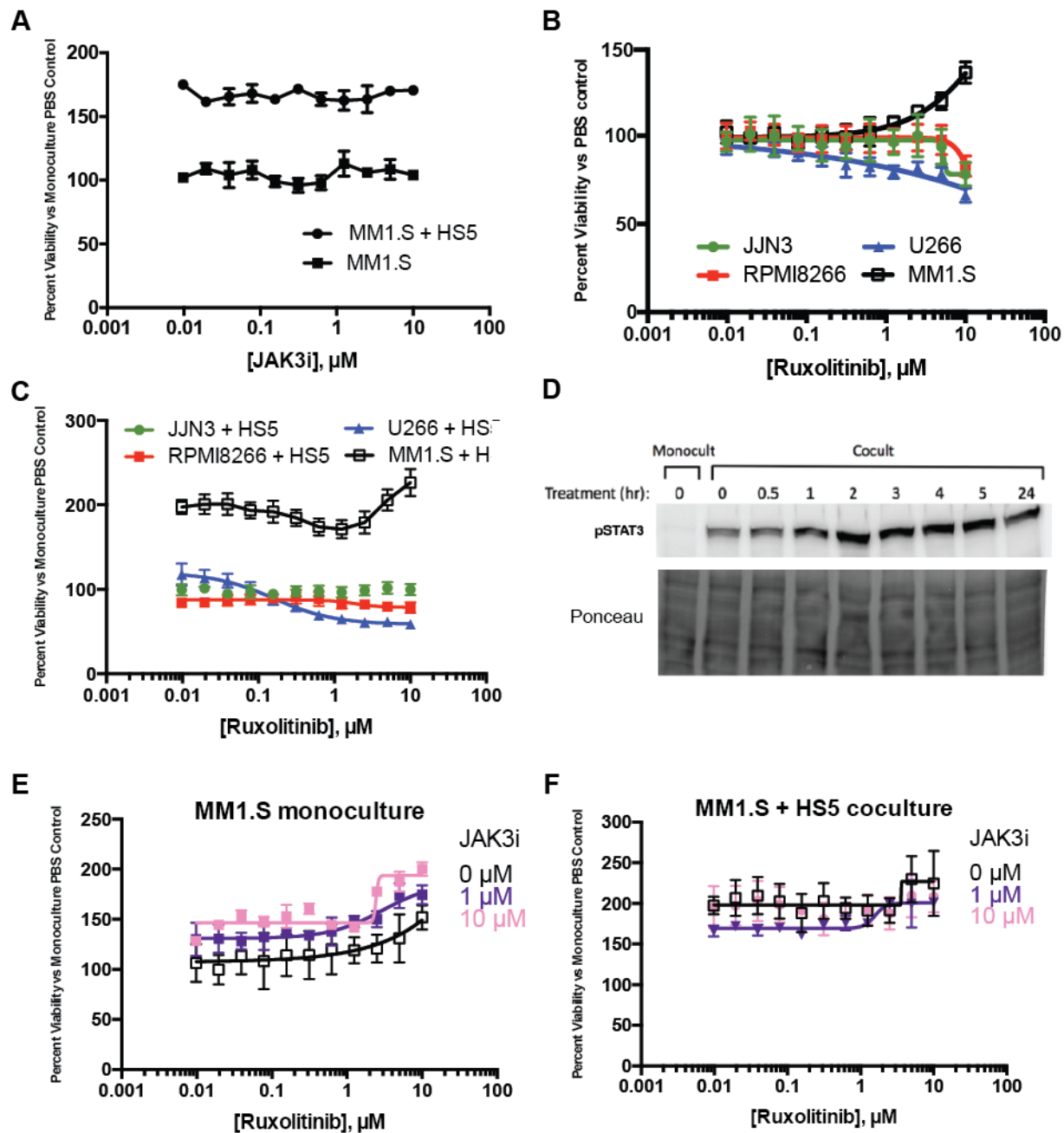
472 phosphorylation is also increased in response to co-culture and rapidly reversed by tofacitinib

473 treatment. **C.** While co-culture increases JAK3 protein expression, there does not seem to be any

474 significant change in signaling via JAK3 after tofacitinib based on phosphorylation status.

475 Western blots are representative of assays performed in biological duplicate.

476

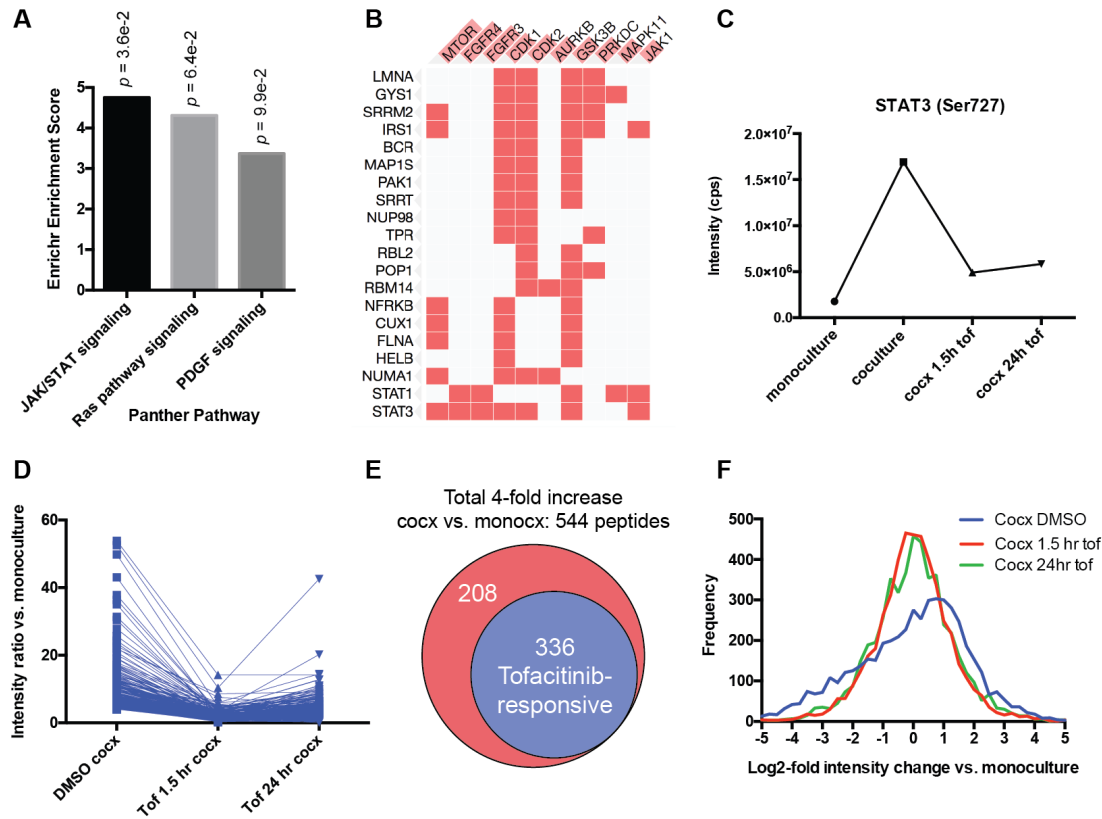


477

478 **Figure 4. Ruxolitinib demonstrates less anti-MM activity than tofacitinib.** A. A highly
 479 selective, irreversible inhibitor of JAK3, JAK3i, does not have any effects on MM.1S either in
 480 mono-culture or in co-culture with HS5. B. The JAK1/2 inhibitor ruxolitinib has minimal anti-
 481 MM effects in monoculture vs. four MM cell lines, and in fact appears to promote growth of
 482 MM.1S at higher concentrations. C. A similar phenomenon is noted in HS5 co-culture. D.

483 Ruxolitinib does not inhibit and in fact increases signaling via STAT3 in MM.1S grown in HS5
484 co-culture. **E.-F.** Combination of ruxolitinib with JAK3i, to achieve simultaneous JAK1/2/3
485 inhibition, does not recapitulate effects of tofacitinib in MM.1S. All error bars represent +/- S.D.
486 from assay performed in quadruplicate in 384-well plates.
487
488

489



490

491 **Figure 5. Unbiased phosphoproteomics reveals that tofacitinib broadly reverses pro-**
 492 **growth signaling from stroma to MM cells.** **A.** Analysis of 4895 phosphorylation sites

493 quantified by LC-MS/MS on biological replicate samples revealed 544 phosphosites to be
 494 upregulated 4-fold in untreated MM.1S in coculture with HS5 vs. monoculture. Of these

495 upregulated phosphopeptides, Panther pathway analysis showed JAK/STAT signaling to be the

496 only significantly enriched pathway ($p = 0.036$). **B.** Kinase Enrichment Analysis demonstrated

497 that many of the upregulated phosphopeptides derive from known substrates of other kinases

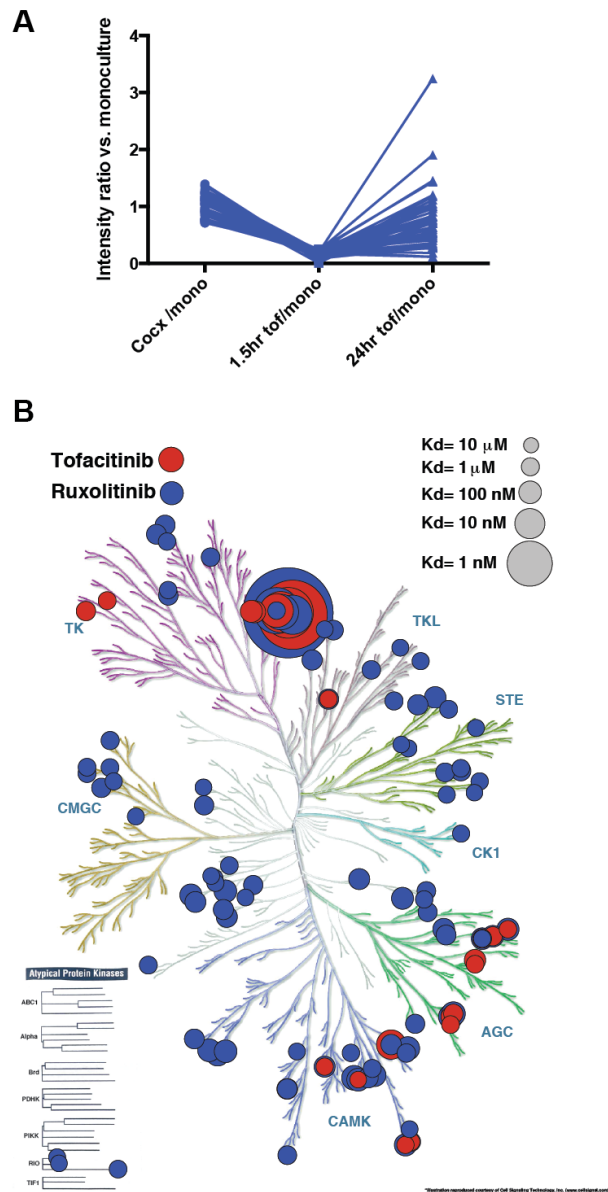
498 related to proliferation such as mTOR, CDK1, and CDK2, as well as JAK1. Phosphorylated

499 protein substrates are on the left and enriched kinases across the top. Length of red bar in kinase

500 name is indicative of strength of enrichment. **C.** Quantitative phosphoproteomic intensity of the

501 JAK-responsive phosphosite Ser727 on STAT3, both in untreated co-culture vs. monoculture,

502 and after tofacitinib treatment, is very similar to the pattern found by Western blotting for the
503 other known-JAK responsive STAT3 phosphosite Tyr707 (Fig. 3A), serving to validate this
504 proteomics approach. **D.** Dynamics of all phosphosites found to be responsive to tofacitinib
505 based on the criteria: 1) increased 4-fold in co-culture vs. monoculture 2) decreased at least-2
506 fold from untreated co-culture after 1.5 hr of 1 μ M tofacitinib treatment and 3) phosphosite
507 intensity remains below the untreated co-culture level after 24h of tofacitinib treatment. **E.** Of
508 544 upregulated phosphopeptides in co-culture, 336 (62%) were defined as being tofacitinib-
509 responsive using the criteria in D. **F.** Examining the global phosphosite intensity across all 4895
510 quantified phosphopeptides demonstrates a general increase in phosphorylation of MM.1S
511 proteins in untreated co-culture with HS5 (“Cocx DMSO”; note shift of distribution maximum to
512 log₂-fold change vs. monoculture of ~1) which is then broadly reversed by tofacitinib treatment.
513 Tof = tofacitinib; monocx = monoculture; cocx = co-culture.
514



515

516 **Figure 6. Phosphoproteomics reveals minimal evidence of tofacitinib off-target effects in**

517 **MM. A.** Only 54 phosphopeptides were identified that met the criteria: 1) <50% intensity

518 change in untreated co-culture vs. monoculture and 2) decreased >4-fold after 1.5 hr tofacitinib

519 treatment. These phosphopeptides showed no significant biological pathway enrichment upon

520 Panther or other bioinformatic analysis by Enrichr, suggesting no prominent off-target effects of

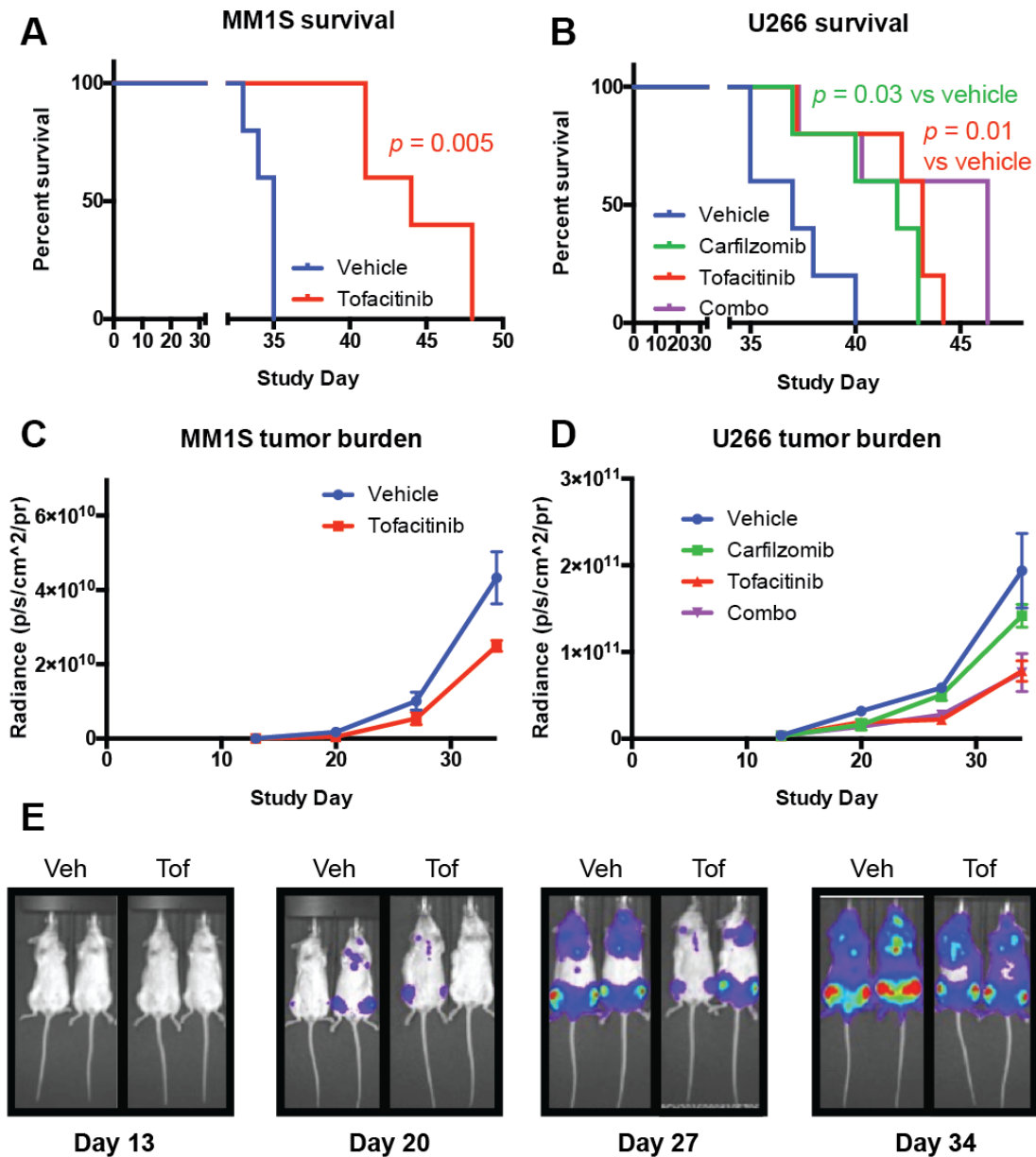
521 tofacitinib in this system. **B.** Cell-free kinase inhibitor activity data from LINCS KINOMEScan

522 database demonstrates that tofacitinib is much more specific for JAK-family kinases (large

523 circles, denoting strong binding, top center) than ruxolitinib, which has off-target activity against
524 many more kinases. Figure rendered using KinomeRender³⁹.

525

526



527

528 **Figure 7. Tofacitinib has anti-MM activity *in vivo*.** Luciferase labeled-MM.1S and U266 MM

529 cell lines were implanted intravenously into NSG mice and tumors allowed to grow for 13 days.

530 Mice were randomized ($n = 5$ mice per arm) and drug dosing was then begun for four weeks.

531 Tofacitinib dose = 21.5 mg/kg/day by subcutaneous pump. Carfilzomib dose = 2 mg/kg IV

532 2x/week for four weeks. **A-B.** Tofacitinib significantly increased survival of NSG mice in these

533 aggressive mouse models of MM by Log-rank test. **C-D.** Bioluminescence imaging for tumor

- 534 burden was performed at Day 13, Day 20, Day 27, Day 34. Error bars represent +/- S.D. **E.**
- 535 Example bioluminescent images from MM.1S study showing prominent localization of tumor
- 536 cells to hindlimb bone marrow.

537 REFERENCES

- 538 1 Manier, S., Kawano, Y., Bianchi, G., Roccaro, A. M. & Ghobrial, I. M. Cell autonomous
539 and microenvironmental regulation of tumor progression in precursor states of multiple
540 myeloma. *Curr Opin Hematol* **23**, 426-433 (2016).
- 541 2 Kuehl, W. M. & Bergsagel, P. L. Molecular pathogenesis of multiple myeloma and its
542 premalignant precursor. *J Clin Invest* **122**, 3456-3463 (2012).
- 543 3 Bianchi, G. & Munshi, N. C. Pathogenesis beyond the cancer clone(s) in multiple
544 myeloma. *Blood* **125**, 3049-3058 (2015).
- 545 4 Gupta, S. C., Sung, B., Prasad, S., Webb, L. J. & Aggarwal, B. B. Cancer drug discovery
546 by repurposing: teaching new tricks to old dogs. *Trends Pharmacol Sci* **34**, 508-517
547 (2013).
- 548 5 Corsello, S. M. *et al.* The Drug Repurposing Hub: a next-generation drug library and
549 information resource. *Nat Med* **23**, 405-408 (2017).
- 550 6 Shim, J. S. & Liu, J. O. Recent advances in drug repositioning for the discovery of new
551 anticancer drugs. *Int J Biol Sci* **10**, 654-663 (2014).
- 552 7 Nosengo, N. Can you teach old drugs new tricks? *Nature* **534**, 314-316 (2016).
- 553 8 Murnane, M. *et al.* Defining Primary Marrow Microenvironment-Induced Synthetic
554 Lethality and Resistance for 2,684 Approved Drugs Across Molecularly Distinct Forms
555 of Multiple Myeloma. *Blood (ASH Abstract)* **126** (2015).
- 556 9 Meyer, D. M. *et al.* Anti-inflammatory activity and neutrophil reductions mediated by the
557 JAK1/JAK3 inhibitor, CP-690,550, in rat adjuvant-induced arthritis. *J Inflamm* **7**, 41
558 (2010).
- 559 10 Shuai, K. & Liu, B. Regulation of JAK-STAT signalling in the immune system. *Nature*
560 *reviews. Immunology* **3**, 900-911 (2003).
- 561 11 Fleischmann, R. *et al.* Placebo-controlled trial of tofacitinib monotherapy in rheumatoid
562 arthritis. *N Engl J Med* **367**, 495-507 (2012).
- 563 12 Klein, B., Zhang, X. G., Lu, Z. Y. & Bataille, R. Interleukin-6 in human multiple
564 myeloma. *Blood* **85**, 863-872 (1995).
- 565 13 Das, R. *et al.* Microenvironment-dependent growth of preneoplastic and malignant
566 plasma cells in humanized mice. *Nat Med* **22**, 1351-1357 (2016).
- 567 14 Rosean, T. R. *et al.* Preclinical validation of interleukin 6 as a therapeutic target in
568 multiple myeloma. *Immunol Res* **59**, 188-202 (2014).
- 569 15 Monaghan, K. A., Khong, T., Burns, C. J. & Spencer, A. The novel JAK inhibitor
570 CYT387 suppresses multiple signalling pathways, prevents proliferation and induces
571 apoptosis in phenotypically diverse myeloma cells. *Leukemia* **25**, 1891-1899 (2011).
- 572 16 Li, J. *et al.* INCB16562, a JAK1/2 selective inhibitor, is efficacious against multiple
573 myeloma cells and reverses the protective effects of cytokine and stromal cell support.
574 *Neoplasia* **12**, 28-38 (2010).
- 575 17 De Vos, J., Jourdan, M., Tarte, K., Jasmin, C. & Klein, B. JAK2 tyrosine kinase inhibitor
576 tyrphostin AG490 downregulates the mitogen-activated protein kinase (MAPK) and
577 signal transducer and activator of transcription (STAT) pathways and induces apoptosis
578 in myeloma cells. *Brit J Hematol* **109**, 823-828 (2000).
- 579 18 Ramakrishnan, V. *et al.* TG101209, a novel JAK2 inhibitor, has significant in vitro
580 activity in multiple myeloma and displays preferential cytotoxicity for CD45+ myeloma
581 cells. *Am J Hematol* **85**, 675-686 (2010).

- 582 19 Scuto, A. *et al.* The novel JAK inhibitor AZD1480 blocks STAT3 and FGFR3 signaling,
583 resulting in suppression of human myeloma cell growth and survival. *Leukemia* **25**, 538-
584 550 (2011).
- 585 20 Burger, R. *et al.* Janus kinase inhibitor INCB20 has antiproliferative and apoptotic effects
586 on human myeloma cells in vitro and in vivo. *Mol Cancer Therap* **8**, 26-35 (2009).
- 587 21 McMillin, D. W. *et al.* Tumor cell-specific bioluminescence platform to identify stroma-
588 induced changes to anticancer drug activity. *Nat Med* **16**, 483-489 (2010).
- 589 22 Smith, E. J. *et al.* A novel, native-format bispecific antibody triggering T-cell killing of
590 B-cells is robustly active in mouse tumor models and cynomolgus monkeys. *Sci Rep* **5**,
591 17943 (2015).
- 592 23 Wiita, A. P. *et al.* Global cellular response to chemotherapy-induced apoptosis. *eLife* **2**,
593 e01236 (2013).
- 594 24 Anders, S. & Huber, W. Differential expression analysis for sequence count data.
595 *Genome Biol* **11**, R106 (2010).
- 596 25 Kuleshov, M. V. *et al.* Enrichr: a comprehensive gene set enrichment analysis web server
597 2016 update. *Nucleic Acids Res* **44**, W90-97 (2016).
- 598 26 Fila, J. & Honys, D. Enrichment techniques employed in phosphoproteomics. *Amino*
599 *Acids* **43**, 1025-1047 (2012).
- 600 27 Cox, J. & Mann, M. MaxQuant enables high peptide identification rates, individualized
601 p.p.b.-range mass accuracies and proteome-wide protein quantification. *Nat Biotechnol*
602 **26** (2008).
- 603 28 Lachmann, A. *et al.* ChEA: transcription factor regulation inferred from integrating
604 genome-wide ChIP-X experiments. *Bioinformatics* **26**, 2438-2444 (2010).
- 605 29 Mi, H. *et al.* PANTHER version 11: expanded annotation data from Gene Ontology and
606 Reactome pathways, and data analysis tool enhancements. *Nucleic Acids Res* **45**, D183-
607 D189 (2017).
- 608 30 Nelson, E. A., Walker, S. R. & Frank, D. A. in *Advances in Biology and Therapy of*
609 *Multiple Myeloma: Volume 1: Basic Science* (ed N.C. Munshi and K.C. Anderson) Ch.
610 7, 117-138 (Springer, 2013).
- 611 31 Jernberg-Wiklund, H., Pettersson, M., Carlsson, M. & Nilsson, K. Increase in interleukin
612 6 (IL-6) and IL-6 receptor expression in a human multiple myeloma cell line, U-266,
613 during long-term in vitro culture and the development of a possible autocrine IL-6 loop.
614 *Leukemia* **6**, 310-318 (1992).
- 615 32 Smith, G. A., Uchida, K., Weiss, A. & Taunton, J. Essential biphasic role for JAK3
616 catalytic activity in IL-2 receptor signaling. *Nat Chem Biol* **12**, 373-379 (2016).
- 617 33 Quintas-Cardama, A. *et al.* Preclinical characterization of the selective JAK1/2 inhibitor
618 INCB018424: therapeutic implications for the treatment of myeloproliferative neoplasms.
619 *Blood* **115**, 3109-3117 (2010).
- 620 34 Leitner, A. Enrichment Strategies in Phosphoproteomics. *Methods Mol Biol* **1355**, 105-
621 121 (2016).
- 622 35 Lachmann, A. & Ma'ayan, A. KEA: kinase enrichment analysis. *Bioinformatics* **25**, 684-
623 686 (2009).
- 624 36 Yokoyama, S. *et al.* Janus Kinase Inhibitor Tofacitinib Shows Potent Efficacy in a Mouse
625 Model of Autoimmune Lymphoproliferative Syndrome (ALPS). *J Clin Immunol* **35**, 661-
626 667 (2015).

- 627 37 Zlei, M. *et al.* Characterization of in vitro growth of multiple myeloma cells. *Exp*
628 *Hematol* **35**, 1550-1561 (2007).
- 629 38 Curtis, J. R. *et al.* Tofacitinib, an oral Janus kinase inhibitor: analysis of malignancies
630 across the rheumatoid arthritis clinical development programme. *Ann Rheum Dis* **75**, 831-
631 841 (2016).
- 632 39 Chartier, M., Chenard, T., Barker, J. & Najmanovich, R. Kinome Render: a stand-alone
633 and web-accessible tool to annotate the human protein kinome tree. *PeerJ* **1**, e126 (2013).
634